Ignition of pre-compressed targets by fast electrons

J.J. Honrubia[1] and J. Meyer-ter-Vehn[2]

[1] *GIFI, Universidad Politécnica, Madrid, Spain*

[2] *Max-Planck-Institut für Quantenoptik, Garching, Germany*

1. Introduction.

The success of fast ignition by laser-driven electrons relies on a good coupling of the electron beam to the compressed fuel. In cone guided targets [1], the coupling efficiency depends, among other parameters, on the distance from the cone tip to the dense core and on the initial divergence of the relativistic electron beam. Here, we investigate fast electron energy deposition, beam coupling and target ignition by means of integrated simulations including 2D/3D hybrid PIC electron transport [2, 3], hydrodynamics, fusion reactions and α-particle transport. The study has been motivated by the future fast ignition facilities [4].

2. Imploded target configuration and beam parameters.

The configuration of the imploded DT core used here is shown in Fig. 1. It consists of a super-Gaussian spherical blob with a peak density of 400 g/cm^3 and a full-width-at-half-maximum (FWHM) of 82 μm sited on a low density *halo* (1.5 g/cm^3). The distance *d* from the cone tip to the dense blob is considered as a parameter ranging from 75 to 150 μm. The imploded DT core is heated by a fast electron beam with a mean kinetic energy of 2 MeV and an initial divergence half-angle θ = 22.5º (FWHM) taken from the cone target experiments reported in [1]. We have also considered the cases of θ = 30º and 40º to check the sensitivity of core heating to the beam divergence. The pulse duration vary from 10 to 20 ps and the total energies from 24 to 58 kJ depending on the distance *d* and the divergence angle θ.

Fast electron energy deposition is computed with the hybrid model shown in [3], which solves the relativistic Fokker-Planck equation and takes into account self-generated fields. Resistivities are computed from the classical Spitzer model and plasma properties are taken from two-temperature SESAME equation of state.

The energy deposition by 2.2 MeV electrons impinging perpendicularly on a DT slab obtained with the present model is shown in Fig. 2a. Notice that the beam is collimated in the first half of the range, being subject to scattering and beam *blooming* in the second half. Notice also and that the range obtained is similar to that found by other authors [5]. Figure 2b shows that the energy deposition pattern changes substantially for electrons with realistic energy and angular distributions, leading to the apparent range '*lenthening*' shown in the figure.

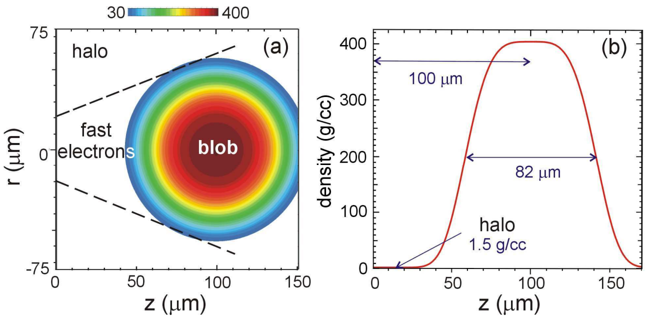

FIG. 1. Central cut through imploded target configuration: (a) density isocontours in g/cm^3 and (b) density profile at r = 0.

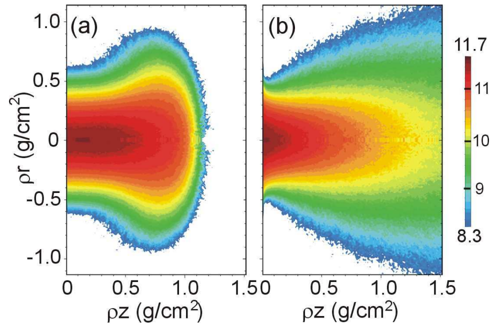

FIG. 2. Energy deposition isocontours of (a) 2.2 MeV electrons impinging perpendicularly on a DT slab and (b) electrons with a mean energy of 2.2MeV and a divergence angle of 22º.

3. Fast electron energy deposition

In the lower density region, ohmic heating due to return currents is the dominant energy deposition mechanism. Here, field generation is suppressed due to high electron temperatures and low resitivities and beam electrons propagate with approximately the initial divergence angle. At densities of tens of g/cm^3, higher plasma resistivities lead to enhanced field generation and beam collimation by the self-generated azimuthal magnetic field [3]. Beam collimation turns out to be important for core heating due to the reduction of the beam angular spread. Notice in Figs. 3a and b how the beam collimation increases the peak energy density deposited by a factor of 2. It is consistent with the resistive collimation model developed by Bell and Kingham [6], which predicts collimation for the beam parameters considered here, even for the case of θ = 40º. In the dense core, the DT heating is almost exclusively due to Coulomb energy deposition and collective effects play only a minor role at so high densities. The temperature profile at the end of the heating pulse is shown in Fig. 3c.

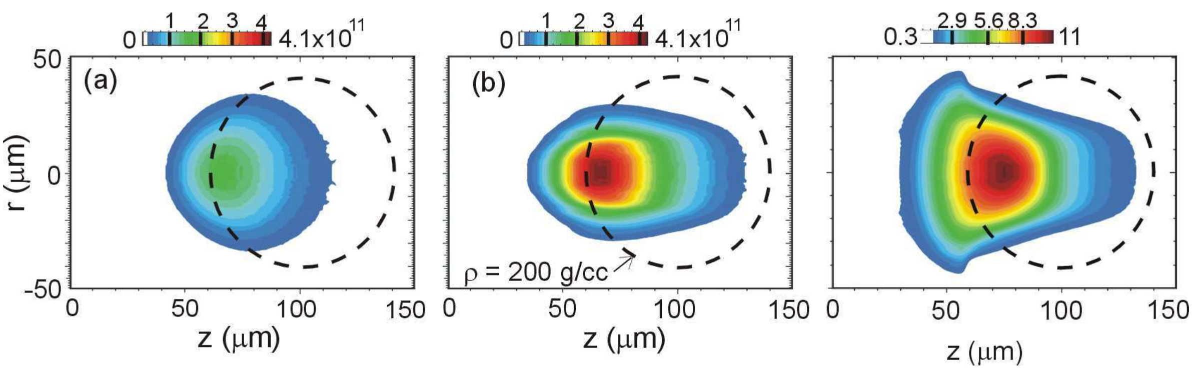

FIG. 3. Comparison of the energy density (in J/cm^3) deposited by the fast electron beam with an initial divergence of 22º (FWHM): (a) simulation with self-generated fields artificially suppressed and (b) full simulation. (c) Ion temperature distribution in keV at the end of the pulse in the case (b). Dashed circles show the initial density contour of 200 g/cm^3.

4. Coupling efficiency and DT ignition.

The beam coupling efficiencies, defined here as the energy fraction of the electron beam deposited at densities higher than 200 g/cm^3, predicted by our integrated calculations are depicted in Fig. 4a. Notice that the sensitivity of the coupling efficiency to the distance d is more pronounced for large beam divergences. Assuming a laser-to-fast electron conversion efficiency of 40% and a minimum overall coupling efficiency of 25% for feasible fast ignition schemes [7], one finds that a suitable scheme has to have a minimum electron beam coupling efficiency about 0.6. We can see in Fig. 4a that only imploded configurations with distances d lower than 130 and 80 μm for divergence angles of 22º and 30º, respectively, are suitable, while initial divergences of 40º or higher give too low overall coupling efficiencies. The important role played by beam collimation is also shown in Fig. 4a. If beam-generated fields are not taken into account, overall coupling efficiencies of the order of 25% are obtained only for targets with distances d lower than 75 μm, which may be too short from the cone target compression hydrodynamics viewpoint.

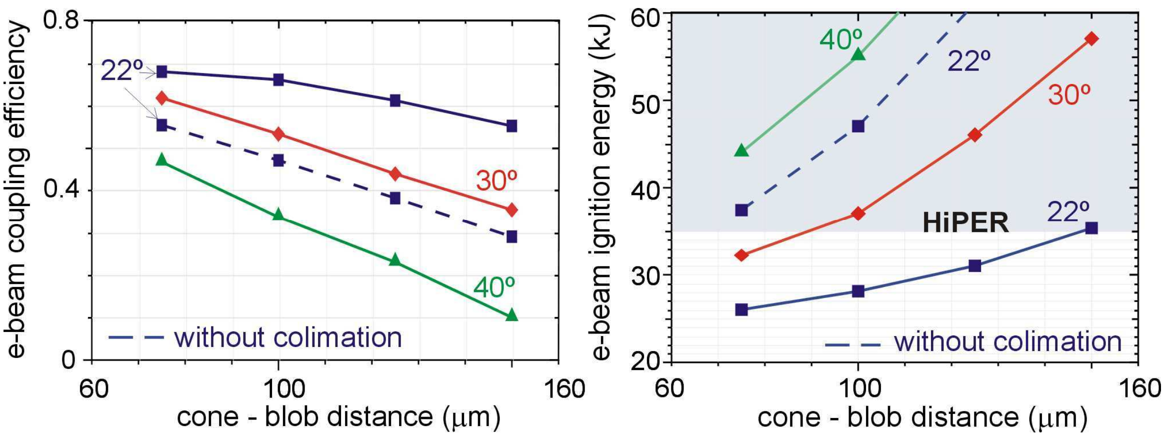

FIG. 4. (a) Electron beam coupling efficiency as a function of the cone-blob distance. Curves labeled with squares correspond to the initial divergence half-angle of the fast electrons of 22º (FWHM), the curve labeled with diamonds to a divergence of 30º (FWHM), and the curve labeled with triangles to 40º (FWHM). The dashed line shows the coupling efficiency when the self-generated fields are artificially suppressed. (b) Ignition energies obtained with the model discussed in the text.

We have performed simulations to estimate the ignition energies as a function of cone – blob distance and initial divergence angle. Results are plotted in Fig. 4b. It is worth remarking the very important dependence of the ignition energy on both parameters, which are crucial for fast ignition. Our model predicts that the imploded target configuration of Fig. 1 heated by rather collimated electron beams (θ = 22º) will ignite with energies between 26 and 35 kJ. The corresponding laser energies can be estimated as 65 and 88 kJ, respectively. If self-generated fields are artificially suppressed, we find that the ignition energies are much higher, even unreachable for 60 – 70 kJ laser beams.

5. Conclusions.

Integrated simulations show that collective effects play a role for core heating improving the coupling efficiency substantially via beam collimation. Simulations also evidence a large dependence of the ignition energy on the distance between the cone tip and the dense blob and the initial beam divergence angle. Since these parameters depend, respectively, on details of specific target designs and on the interaction of short pulses with the cone not fully explored yet, we have made a parametric study to estimate the ignition energies for different parameter sets. If plasma instabilities at densities lower than 1.5 g/cm^3 are not relevant and electron beams emerge from the cone tip with a divergence angle similar to that measured in experiments with cone targets [1], 25 – 30 kJ electron beams will be able to ignite imploded DT targets. Those beams could be generated with the short-pulse laser proposed for HiPER [4]. However, detailed studies about the configuration of the imploded core and the electron beam generated by the interaction of 10 – 20 ps laser pulses with cones are still necessary.

Acknowledgements

This work was supported by the research grant ENE2006-06339 of the Spanish Ministry of Education and by the Association EURATOM - IPP Garching in the framework of IFE Keep-in-Touch Activities and the Fusion Mobility Programme.

References

[1] R. Kodama et al., *Nature* **412**, 798 (2001); R. Kodama et al. *Nature* **418**, 933 (2002); and R.B. Stephens et al., *Phys. Rev. Lett.* **91**, 185001 (2003).

[2] J. Meyer-ter-Vehn et al., *Plasma Phys. Control. Fus.* **47**, (2005)

[3] J.J. Honrubia and J. Meyer-ter-Vehn, *Nucl. Fusion* **46**, L25 (2006).

[4] M. Dunne, *Nature Physics* **2**, 2 (2006) and H. Azechi et al., *Plasma Phys. Control. Fusion* **48,** B267 (2006).

[5] C.K. Li and R.D. Petrasso, *Phys. Plasmas* **13**, 056314 (2006); M. Tabak et al., *Phys. Plasmas* **12**, 052708 (2005); and C. Deutsch et al., *Phys. Rev. Lett.* **77**, 12 (1996).

[6] A.R. Bell and R.J. Kingham, *Phys. Rev. Lett.* **91**, 035003 (2003).

[7] S. Atzeni et al., *Phys. Plasmas* **1**, (2006).